Effects of *Acuc* on the Growth Development and Spinosad Biosynthesis of *Saccharopolyspora Spinosa*

Zhudong Liu
Hunan Normal University
Jie Xiao
Hunan Normal University
Jianli Tang
Hunan Normal University
Yang Liu
Hunan Normal University
Ling Shuai
Hunan Normal University
Li Cao
Hunan Normal University
Ziyuan Xia
Hunan Normal University
Xuezhi Ding
Hunan Normal University
Jie Rang
Hunan Normal University
Liqiu Xia (xialq@hunnu.edu.cn)
Hunan Normal University https://orcid.org/0000-0001-8443-2916

Research Article

Keywords: Saccharopolyspora spinosa, spinosad, acetoin utilization protein, knockout, overexpression, comparative proteomics

Posted Date: March 22nd, 2021

DOI: https://doi.org/10.21203/rs.3.rs-331603/v1

Version of Record: A version of this preprint was published at Microbial Cell Factories on July 22nd, 2021. See the published version at https://doi.org/10.1186/s12934-021-01630-2.

Abstract

Background: The interaction between *acuC* and spinosad biosynthesis is complex. In this study, acetoin utilization protein (*acuC*) was characterized. It is a type I histone deacetylase that is highly conserved in bacteria. This study first explored the effect of *acuC* on the growth and development of secondary metabolites of *S. spinosa*.

Results: The knockout strain and overexpression strain were constructed separately with the shuttle vector pOJ260. The overexpression of the *acuC* gene affects the growth and phenotype of *S. spinosa.* Moreover, the spore production ability of the *S. spinosa-acuC* strain on solid medium was weaker than that of the wild-type strain. HPLC analysis of the fermentation products for the wild-type and mutant strains demonstrated that the yield of the overexpression strain was 87% higher than that of the wild-type strain.

Conclusions: We concluded that the overexpression of *acuC* positively regulated the biosynthesis of spinosad and affected the acetylation pathway and the growth of *S. spinosa*. A comparative proteomic analysis between the wild-type and overexpression strains revealed related genes in different metabolic pathways that were affected. We envision that these results can be extended to other actinomycetes for secondary metabolite improvement.

Highlight

1. The overexpression of gene *acuC* in *spinosa* exerted positive impacts on spinosad accumulation in comparison with the wild-type strain.
2. The overexpression of *acuC* led to the activation of acetylated Acs protein, which promoted the biosynthesis of acetyl-CoA, which acts as a substrate of spinosyn biosynthesis.
3. Proteomics analysis was applied on wild-type and *acuC* overexpression strain to investigate the mechanism of spinosad biosynthesis for the first time.

1 Background

Saccharopolyspora spinosa is a gram-positive bacterium that is non-acid-resistant and aerobic[1]. Spinosyns are synthesized by fermentation of *S. spinosa* under aerobic conditions[2]; Spinosyns are novel macrolide compounds with high insecticidal activity and can be widely used in crop pests such as *Coleoptera*, *Hymenoptera,* and *Diptera*[3]. It is a promising biopesticide that has strong insecticidal activity and a broad pesticidal spectrum. Spinosad is composed of spinosyn A and spinosyn D, which has no negative effects and very low toxicity on nontarget insects and mammals, do not cause environmental pollution and exhibit both the efficiency of chemical pesticides and the safety of biological pesticides, compared with that of traditional chemical pesticides[4,5,6]. However, the yield of spinosad is too low to meet the needs of industrial production, and the fermentation time is long for the wild type, which limits the popularization and application of spinosad[7].

Posttranslational modifications (PTMs) of proteins are parts of significant regulatory mechanisms that widely exist in all organisms, and they include methylation, glycosylation, phosphorylation, acetylation, alkylation and biotinylation. PTMs can endow new functions and properties to the modified proteins, including enzyme activity, subcellular localization, interactions with molecular chaperones, stability and DNA binding changes.

The acetylation levels of proteins are controlled by an acetylase and a deacetylase, and the acetylase catalyzes acetyl group transfer from acetyl-CoA to the substrate protein during translation. However, the function of deacetylase is the opposite; it removes the acetyl group from an acetylated protein. Two main types of deacetylases are involved in this process, zinc-dependent (mainly histone deacetylases) and NAD-dependent deacetylases, which mainly play a role in the metabolic process.

In 1996, the first histone deacetylase was found[8]. Histone acetylation/deacetylation extensively occurs in the genetic material of natural organisms and serves as an important biological information regulator. Histone deacetylases are members of an ancient group of enzymes that are widely present in plants, animals and microorganisms and have also been found in archaebacteria and eubacteria[9]. Currently, HDACs are classified into two families: the NAD-dependent sirtuin family and the traditional HDAC family[10].

The acetylation of acetyl-CoA synthetase of *S. coelicolor* is regulated in vivo, but the acetyl transferase responsible for its acetylation has not been identified[14]. A gene homology analysis found two homologous genes in *S. erythraea*: the SACE3798 gene, which expresses a protein with deacetylation activity, and the SACE5148 gene, which expresses a protein with acetyltransferase activity. The growth cycle of a SACE-3798 knockout strain was longer than that of the wild-type strain. Meanwhile, pigment production in the SACE5148 knockout strain is delayed[15].

Acetoin utilization protein (*acuC*) is a class I deacetylase that exists in only bacteria. In *Bacillus subtilis*, the regulation of deacetylases is more complex. There are two main types of deacetylases: the deacetylase SrtN of the NAD-dependent Sirt family and the deacetylase *acuC* of the NAD-independent family[16]. *acuA* is a homologous gene of acyltransferase identified in *B. subtilis*[17].

To investigate the effects of *acuC* on the morphological differentiation and spinosad synthesis of *S. spinosa*, a fragment of the *acuC* gene was cloned from the genome of *S. spinosa* by PCR amplification, and the *acuC* gene was simultaneously placed under the strong promoter $P_{ermE.}$ Then, the knockout vector pOJ260-Δ*acuC* and the overexpression vector pOJ260-P_{ermE}-*acuC* were constructed by using digestion and ligation methods. The knockout vector pOJ260-Δ*acuC* was introduced into the *S. spinosa* genome by conjugative transfer to block the expression of the *acuC* gene. The overexpression vector pOJ260-P_{ermE}-*acuC* was introduced into the *S. spinosa* genome by conjugative transfer to overexpress the *acuC* gene with the same method.

This research provides a novel bioinformatic study of the gene functions involved in the acetylation pathway in *S. spinosa*. Through differential proteomics analysis, we classified differential proteins in different metabolic pathways. This work also provides a basis for exploring the antibiotic biosynthesis metabolic regulation network in actinomycetes.

2 Results

2.1 Effects of knockout and overexpression of *acuC* on morphology and sporulation

To study the differences in growth between the wild-type and mutant strains in fermentation medium, the growth characteristics were measured and controlled in real time **(Fig. 1)**. The results showed that the logarithmic growth phases of *S. spinosa* and *S. spinosa-acuC* were basically synchronous, and the wild-type and *S. spinosa-acuC* strains entered the stationary growth phase after 60 h. However, the biomass of *S. spinosa-acuC* at the stationary growth phase was higher than that of the wild-type strain. The *S. spinosa*-Δ*acuC* strain entered the stationary growth phase at 84 h and entered the recession phase after 200 h. The biomass of the *S. spinosa*-Δ*acuC* strain was significantly lower than that of the wild-type strain.

These strains were cultured in CSM medium for 48 h and collected. After the samples were treated by gradient dehydration, the morphology of mycelium and development of the wild-type and mutant strains were observed by emission scanning electron microscopy (SEM). The results showed that the mycelium of *S. spinosa*-Δ*acu*C was more slender and shrunken than that of the wild-type strain and that the hyphal length of *S. spinosa*-Δ*acu*C was longer **(Fig. 2A)**. However, the mycelia of *S. spinosa-acu*C were plumper and more fragmented than those of the wild-type strain.

To observe the effect of *acuC* knockout and overexpression on sporulation in different solid culture media, the wild-type and mutant strains were observed on BHI, TSB and CSM solid media **(Fig. 2B)**. The sporulation production capacities of *S. spinosa*-Δ*acuC* and *S. spinosa* were obviously stronger than that of *S. spinosa-acuC* on this three solid media. *S. spinosa-acuC* produced a small number of spores on the CSM medium and hardly produced on TSB and BHI media. This phenomenon lasted the whole incubation period. To explain the low spore production of *S. spinosa-acuC*, we measured the expression of the sporulation-specific genes *whiA* and *ssgA* and the mycelial division-related gene *bldD* by qRT-PCR. The expression of *whiA* is related to the synthesis of the white pigment characteristic of mature *S. venezuelae* spores. The *ssgA* was confirmed to be involved in the regulation of the white phenotype. The expression of *whiA* and *ssgA* was downregulated, but the expression of *bldD* was upregulated in *S. spinosa-acuC* **(Fig. 3)**. The results implied that *acuC* indirectly affected the expression of *whiA*, *bldD* and *ssgA*. Therefore, we hypothesized that the *acuC* gene plays a significant role in the regulation of morphology and sporulation.

2.2 Effects of *acuC* knockout and overexpression on spinosad biosynthesis

Spinosyn A and spinosyn D were extracted from fermentation broths of the wild-type and mutant strains and examined by HPLC **(Fig. 4A)**. The peak areas of spinosyns A and D from *S. spinosa* were 216.9 and 36.7, respectively. Their peak areas for *S. spinosa-acuC* were 405.6 and 68.6. In addition, *S. spinosa-*Δ*acuC* produced only a small amount of spinosad. The peak areas of spinosyns A and D from *S. spinosa-*Δ*acuC* were 108.8 and 29.7, respectively. The target peaks were collected for mass spectrometry identification. MS showed the $[M+H]^+$ ions at *m/z*=732.5 **(Fig. 4B)**. This observation verified that the substance was the main component of spinosad, which is consistent with previous data. Thus, the overexpression of *acuC* caused an increase in the yields of spinosyns A and D.

2.3 Biological insecticidal activity of the wild-type and mutant strains

The insecticidal activity of the wild-type and mutant strains was assayed by comparing the half lethal time (LT_{50}) values. *H. armigera* was used as the experimental material. The half lethal time (LT_{50}) of *S. spinosa-acuC* was 0.435 d less than that of *S. spinosa***(Table 1)**. On the first day, the survival number of *H. armigera* was basically the same between *S. spinosa* and *S. spinosa-acuC*, and the survival rates were similar. From the next day, the *S. spinosa-acuC* fermentation exhibited stronger toxicity to *H. armigera* than the wild-type strain fermentation. The survival rate was higher for *S. spinosa-*Δ*acuC* than for the wild-type and *S. spinosa-acuC* strains, and this result showed that the insecticidal activity of *S. spinosa-*Δ*acuC* on *H. armigera* was weaker than that of the wild-type strain **(Fig. S3)**. In conclusion, the insecticidal effect of *S. spinosa-acuC* was significantly higher than that of the wild-type strain, and the knockout strain had the worst insecticidal effect.

2.4 Protein expression differences between the wild-type and mutant strains

Whole-cell proteins of the wild-type and two mutant strains were analyzed by SDS-PAGE at different developmental stages. Significantly different protein bands were demonstrated between the wild-type and the overexpression strain at 48 h **(Fig. 5A)**. These differential bands were selected and further studied through 1D-LC-MS/MS. The identified proteins were then categorized by UniProt (www.uniprot.org), and gene ontology (GO) was used to analyze their functions **(Table 2)**. Then, semiquantitative proteomic samples were prepared from the wild-type and overexpression strains and analyzed. Three biological replicates were identified by LC-MS. The proteomics analysis yielded more information. The PAI values of the two strains were calculated. We performed Venn intersection analysis on the data of the wild-type and overexpression strains, filtered the data and chose the research direction on the basis of the intersections. Venn analysis was performed on the genes differentially expressed between wild-type and overexpression strains according to the up- and downregulation in differential data. In**(Fig. 5B)**, the light purple circle represents the fold change value in the overexpression strain compared to the wild-type strain at 48 h (228 upregulated proteins and 127 downregulated proteins), and the light blue circle represents the fold change value of the overexpression strain compared with the wild-type strain at 144 h (478 upregulated proteins and 356 downregulated proteins). The intersection of the two sets of data represents the common differential proteins (18 upregulated and 78 downregulated) of the wild-type and overexpression strains. Thresholds of 1.5-fold and 0.75-fold were used to indicate significantly upregulated and

downregulated protein expression, respectively. Moreover, 18 upregulated proteins and 78 downregulated proteins were discovered **(Fig. 5C)**.

2.5 Significantly differential proteins influenced by the overexpression of *acuC*

The significantly differential genes were subjected to GO enrichment analysis of the functional and metabolic pathways. First, in the classification of biological pathways, there were 423 pathways in GO enrichment assays, and 120 biological pathways (P<0.05) were detected to have significant differences **(Fig. 6A)**; these were mostly involved in the regulation of organic nitrogen compound metabolism, organic nitrogen compound biosynthesis and small molecule metabolism. Second, in the classification of cell component localization, there were 47 pathways in GO enrichment assays, and 27 pathways (P<0.05) were detected with significant differences; these were mostly involved in the transformation of intracellular components, the cytoplasm and cellular components. Finally, in the category of molecular function, there were 255 pathways in GO enrichment assays, and 56 pathways (P<0.05) were detected with significant differences; these were mostly involved in molecular changes related to the main redox enzyme activities. The overexpression of *acuC* caused obvious changes in biological processes and intracellular molecular function **(Fig. 6B)**. A GO enrichment analysis of different genes and KEGG pathway analysis revealed that significantly different proteins were mainly involved in the glycolysis/gluconeogenic, phenylalanine and β-alanine metabolic pathways **(Fig. 6C)**. The functions of the significantly upregulated genes are shown in **Table 3**; these genes were involved in replication, transcription and translation, energy metabolism and amino acid metabolism during spinosad synthesis. In addition, the significantly downregulated genes associated with growth are also shown in **Table 3**.

Discussion

This study is the first to use knockout and overexpression methods to explore the function of the *acuC* gene in *S. spinosa*, and protoplast transformation was used to integrate recombinant plasmids into the genome of *S. spinosa*. To a certain extent, the method overcomes the complicated restriction modification system of actinomycetes. On the basis of our work, we speculated that in *B. subtilis*, *AcuC* deacetylase is needed to maintain a balance between free CoA and acetyl-CoA during acetoin catabolism.

The acetylation of histone proteins is common in organism growth and development. This phenomenon may play an important role in the regulation of gene expression and posttranslational modification of proteins. The *acuC* gene is a part of the acuABC operon and is related to the acetyl-CoA synthetase gene. The *acuC* gene controls acetyl-CoA synthetase activity through acetylation of acetyl Lys549 residues in bacteria. In *Bacillus subtilis*, the production of the *acuA* and *acuC* genes regulates the posttranslational activity of acetyl-CoA synthetase (AcsA). In *S. spinosa*, the *acuC* gene is an important deacetylase that participates in posttranslational regulation. It is hypothesized that the *acuC* gene affects the acetoin catabolism pathway, causes the emergence of multiprotein complexes through deacetylation of different

proteins and indirectly regulates the growth cycle of bacteria, metabolic processes and the synthesis of secondary metabolites.

In this study, *S. spinosa-ΔacuC* and *S. spinosa-acuC* were constructed. Detection of spinosad production by HPLC revealed that the yield from *S. spinosa-acuC* was 187% greater than that from the wild-type strain, whereas *S. spinosa-ΔacuC* produced less spinosad than the wild type. The proteins of the wild-type strain and *S. spinosa-acuC* were extracted, and 18 significantly upregulated genes were found in *S. spinosa-acuC* by semiquantitative proteomic analysis. The functions of these upregulated genes were analyzed by UniProt and KEGG. The functions of two upregulated genes were identified to involve amino acid metabolism. *purH* is a biofunctional purine biosynthetic protein involved in purine metabolism, and *pepB* is an oligopeptidase that degrade peptides. Four upregulated genes associated with energy metabolism were found: the *fabH* gene, a 3-oxoacyl-acyl-carrier-protein synthase enzyme that is primarily involved in the synthesis and metabolism of fatty acids and catalyzes the condensation reaction of fatty acid synthesis by adding two carbonyl acyl acceptors of malonyl-ACP; the *fabG* gene, which encodes 3-oxoacyl-acyl-carrier-protein reductase, which is also involved in the biosynthesis of fatty acids; and the ATP synthase subunit β, which is encoded by the *atpD* gene. The *atpD* gene participated in oxidative phosphorylation, which was accompanied by the production of ATP from ADP in the presence of a proton gradient on the membrane. Fructose diphosphate aldolase was encoded by the *Fba* gene **(Table 3).**

In this study, the *S. spinosa-acuC* strain had a higher biomass than the wild-type strain. However, it hardly sporulated on TSB and BHI medium, and only a small number of spores were produced on CSM medium. The gene expression levels of the spore germination-related genes *ssgA* and *whiA* were significantly increased in the overexpression strain, which proved this phenomenon. In addition, according to the semiquantitative proteomic analysis, 78 significantly downregulated genes were found in *S. spinosa-acuC*. Three genes were involved in the regulation of growth and development, and their functions were analyzed by UniProt and KEGG software. The *ahpE* gene encoded alkyl hydroperoxide reductase E, which acts as an antioxidative stress regulator in cell protection by detoxifying peroxisomes, but the expression of this gene was significantly decreased in *S. spinosa-acuC*. The *ftsZ* gene is an essential cell division protein that forms a contractile ring structure (Z ring) at future cell division sites. The regulation of ring assembly controls the timing and location of cell division. The ftsZ ring recruits other cell division proteins in the septum to produce a new cell wall between the dividing cells, which regulates cell growth and death during cell development. The *clpC* gene encodes the ATP-dependent Clp protease ATP-binding subunit, which is a necessary regulator for the growth of cells and organisms at high temperatures. The results of the semiquantitative proteomic analysis also proved that overexpression of *acuC* reduces sporulation ability on solid medium.

Then, we summarized the effect of *acuC* in the acetoin catabolism pathway. The overexpression of the *acuC* gene activated the acetylated Acs protein and promoted the production of acetate, which further affected the biosynthesis of acetyl-CoA and provided a large number of precursors for spinosad biosynthesis **(Fig. 7)**.

In this research, the overexpression of *acuC* increased the secondary metabolite product levels and led to the activation of acetylated Acs protein, which promoted the biosynthesis of acetyl-CoA, which acts as a substrate of spinosyn biosynthesis. The measurement of acetyl-CoA contents between the wild-type and overexpression strains at 48 h, 96 h and 192 h also confirmed this result **(Fig. S4)**.

Our study enhanced the current understanding of the metabolic and developmental functions of *acuC* via deletion and overexpression and showed that *acuC* encodes an important protein that could be responsible for secondary metabolites in antibiotic-producing actinomycetes.

Conclusions

Overall, based on the proteomic analysis between the wild-type and mutant strains, the function of *acuC* was identified as a key role in the acetoin catabolism pathway. By choosing the genes related to the cell division and the spore germination, the overexpression of acuC in *S. spinosa* was showed positive impacts on the expression of bldD. The peak areas of spinosyns A and D in *acuC* overexpresson strain reached 405.6 and 68.6, respectively. This research indicated the application of gene overexpression strategy based on the proteomic analysis would be very effective for the rational design of secondary metabolites production improvement.

3 Methods

3.1 Strains, plasmids and growth conditions

The strains and plasmids used in this study are listed in **Table S1** and primers are listed in **Table S2**. The spores of *S. spinosa* were cultivated in CSM activation media (10 g/L glucose; 45 g/L trypticase soy broth; 9 g/L yeast extract; 2.2 g/L $MgSO_4{\cdot}7H_2O$) in a 300 mL flask, with a starting volume of 50 mL at 30 °C with 300 rpm. After cultivation of the strains for 48 h, 3 mL bacteria solution add to 30 mL fementation media (1 g/L KNO_3; 0.01 g/L $FeSO_4$; 0.5 g/L $K_2HPO_4{\cdot}3H_2O$; 0.5 g/L $MgSO_4{\cdot}7H_2O$; 20 g/L glucose; 4 g/L yeast extract; 4 g/L tryptone; pH=7.2) and incubated at 30 °C with 300 rpm. The culture condition of the *S. spinosa-*Δ*acuC* and *S. spinosa-acuC* is the same as the wild-type strain with antibiotic in medium (apramycin, 50 mg/L). The conjugative transfer and protoplast transformation between *E. coli* and *S. spinosa* by using R6 medium (200 g/L sucrose; 10 g/L Dextrin; 26 g/L BHI; 1 g/L Casamino acid; 0.1 g/L K_2SO_4; 0.05 g/L $FeSO_4{\cdot}7H_2O$; 0.05 g/L $MgSO_4{\cdot}7H_2O$; 0.001 g/L $MnCl_2{\cdot}4H_2O$; 0.001 g/L $ZnSO_4{\cdot}7H_2O$; 0.01 mol MOPS; 0.048 mol $CaCl_2$; 0.065 mol L-glutamic acid; 2% agar powder). Then incubated at 30 ℃ for 5-7 days. The yield of spinosad was detected in the initial fermentation medium by HPLC (60 g/L Glucose; 5 g/L Bean cake powder; 7 g/L corn syrup; 22.5 g/L cottonseed meal; 10 g/L soluble starch; 2 g/L yeast powder; 20 mL butyl oleate; 5 g/L $CaCO_3$; 2.5 mL trace elements; pH=7.2-7.4), and incubated at 30 °C with 300 rpm, 10-12 d. The spore morphology of *S. spinosa* was observed in BHI (38 g/L BHI, 2% agar powder), CSM and TSB (tryptic soy broth medium) and incubated at 30 ° C for 6 days. All strains of *E. coli*

were grown in lysogeny broth medium at 37 °C supplemented with antibiotic as required (apramycin, 50 mg/L).

3.2 Construction and verification of the mutant strains

To produce the knockout vector pOJ260-Δ*acuC*, we amplified the *acuC* sequence from the genome of *S. spinosa* CCTCC M206084 with the primer pair *acuC*-F and *acuC*-R (Sangon, Shanghai, China). Then the fragment was digested with *Hin*d and *Eco*R I and ligated into the corresponding restriction sites of pOJ260. Recombinant vector was constructed by T4 ligase-linking the fragment and pOJ260 after the*Hin*d - and *Eco*R I- enzyme digestion **(Figure S1)**. To confirm the successful knockout of the *acuC* fragment, we amplified Apr and *acuC* fragments in the mutant strains genomes with the primer pairs Apr-F/Apr-R and *acuC* -F/*acuC* -R **(Figure S1)**.

The P_{ermE} gene was amplified by the primer pair perm-F/perm-R from pOJ260-*cm*-$P_{ermE}$and the *acuC* gene was amplified by the primer pair *acuC*-F/*acuC*-R from the genome of *S. spinosa.* The fragments were fused by overlap extension PCR by primer pair perm-F/*acuC*-R. Recombinant vector pOJ260-P_{ermE}-*acuC* was constructed by T4 ligase-linking the fused fragment and pOJ260 after the *Hin*d - and *Eco*R -enzyme digestion **(Figure S2)**. To confirm the pOJ260-P_{ermE}-*acuC* was successfully inserted into the chromosome, we amplified the fragment in the mutant strain genome with the primer pair P_{ermE}-F and *acuC*-R. The wild-type genomic and pOJ260-P_{ermE}-*acuC* were used as the positive and negative controls, respectively **(Figure S2)**.

3.3 Cultivation profile analysis of the wild-type and mutant strains

To monitor the growth profiles of wild-type and mutant strains, cells were collected randomly for the growth curve measurement. Optical density at 600 nm (OD_{600}) was used to determine the cell concentration during fermentation. After 48 h of cultivation in CSM medium, 40 μL of wild-type and mutant strains were streaked on BHI, CSM and TSB solid media respectively and incubated at 30 °C for 5 days. Taking the same amount of wild-type and mutant strains into 50 mL CSM liquid medium under the condition of 30 °C and 300 rpm for 2 days. Then, observed the cell morphology by Hitachi SU8010 cold field emission scanning electron microscopy[19],[20]. After fermentation for 10 days, 500 uL fermentation supernatants of the wild-type and mutant strains were extracted with the equal volume of ethyl acetate for 1 h. The supernatant was evaporated and added 50 μL methanol, centrifuged at 10,000 rpm for 5 min, and the ethyl acetate layer was identified by HPLC (Agilent 1290, wavelength: 250 nm, C18 column: AQ12S05-1546, YMC, Japan)[21]. Each sample was loaded onto a C18 column and eluted with the elution buffer at 1.0 mL/min. The elution buffer A: 10% (v/v) acetonitrile; The elution buffer B: 90% (v/v) acetonitrile[22].

3.4 Insecticidal activity and acetyl-coenzyme A (AcCoA) measurement of the wild-type and mutant strains

Fermentation supernatants of the wild-type and mutant strains (1 mL) were added into 20 mL of feed (per liter: 40 g of yeast extract, 70 g of bean flour, 5 g of vitamin C, 15 g of agar, 36% acetic acid, and 10 g of penicillin; whisked until smooth and creamy). The biological activity of the cell culture liquid was measured in 24-well culture plates with one *H. armigera* worm per well; these were cultured at 30 °C with three repeats in parallel, and the mortality rate was determined every 24 h. Uninoculated fermentation medium was used as a negative control. The acetyl-CoA content was determined in total or cytosolic fractions using the Acetyl-Coenzyme A Assay Kit (MAK039-1KT, Sigma-Aldrich) according to the manufacturer's instructions. The sample was then diluted with a reaction mix, and fluorescence was measured using a plate reader and the following settings: λex=535 nm and λem=587 nm. An acetyl-CoA standard curve was made in the range of 10–1000 pmol, and the correlation coefficient was 0.990. The concentrations of the standard solutions used to generate the standard curve were 25 pmol/L, 50 pmol/L, 100 pmol/L, 200 pmol/L, and 400 pmol/L.

3.5 Protein extraction and SDS-PAGE analysis

Cells were harvested (9000 rpm, 10 min, 4 °C) at 48 h from the wild-type and mutant strains washed four times with PBS (10 mM, pH=7.8, precooled at 4 °C). The cell pellet was then resuspended in 200 μL of lysozyme (100 mg/mL), 600 μL of lysis buffer was added to each tube, and ultrasonic fragmentation (JY92 ultrasonic cell grinder, Ningbo new Chi biotechnology company) was used to extract the whole cell protein. Lysis buffer for protein extraction contained 8 M urea, 2 M thiourea, 4% (w/v) CHAPS, 75 mM NaCl, 50 mM Tris-HCl (pH=8.0), 2 mM phenylmethylsulfonyl fluoride and 4 μL of a protease inhibitor cocktail powder (P8465, Sigma, St. Louis, MO, USA). After quantitative analysis of the protein by Bradford assay, the samples were checked by SDS-PAGE before proceeding with LC-MS/MS analysis. For SDS-PAGE analysis, proteins from cell lysates (20 μg of total protein of each phase) were separated from 4 to 12% NuPAGE gels (Invitrogen, Carlsbad, CA, USA), stained with Coomassie brilliant blue (CBB) for 3 h and destained overnight[23].

3.6 LC-MS/MS analysis

Samples were prepared from three biological replicates from wild-type and mutant strains. Tryptic peptides were desalted and concentrated on an Oasis HLB sample cartridge column (Waters Corporation, MA, USA). The purified peptides were dried at 37 °C by vacuum freeze drying (Thermo Fisher, San Jose, CA, USA). The LC-MS/MS analysis was performed on LTQ-XL mass spectrometer (Thermo Fisher, San Jose, CA, USA) coupled with a homemade nano-ionization source, two Finnigan quaternary pumps (a sample pump and an MS pump; LC Packings, San Jose, CA) and an autosampler (LC Packings, San Jose, CA) equipped with a two-position, ten-port valve with a 25-μL sample loop. For proteomic analysis, 20 μL of the redissolved digested peptides (50-μg samples) was first separated by an SCX column (BioBasic SCX, Thermo Fisher, San Jose, CA, USA) with ten concentration steps of ammonium chloride (0, 25, 50, 100, 150, 200, 250, 300, 500 and 1000 mM NH4Cl dissolved in a buffer containing 4 % acetonitrile and 0.1 % formic acid) and then further separated by an RP column (BioBasic C18, Thermo Fisher, San Jose,

CA, USA) as described previously. The elution buffer A was 0.1% formic acid in double-distilled water, and the elution buffer B was 0.1% formic acid in acetonitrile. For the MS detection, the mobile phase was 98% buffer A and 2 % buffer B for the first 5 min, a gradient of 45 min in 40 % buffer B, a gradient of 30 min in 90 % B and 20 min in 98 % buffer A to re-equilibrate the columns at a constant flow rate of 150 μL/min. The LTQ-XL mass spectrometer was operated using the “instrument method” of the Xcaliber software (Thermo Finnigan, San Jose, CA, USA). The temperature of the heated capillary was 180 ℃. The full MS scan ranged from 80 m/z to 2000 m/z, followed by MS/MS analysis in the positive mode and intervening MS/MS scans on the ten most intense ions. Parent ions were selected by dynamic exclusion with a repeat count of two, a repeat duration of 30 s and an exclusive duration of 90 s.

The protein database was downloaded from the National Center of Biotechnology Information (NCBI, http://www.ncbi.nlm.nih.gov/) and contained 6690 entries of *S. spinosa*. Database searches depended on the SEQUEST search engine (Proteome Discoverer 1.3 software package, Thermo Fisher, San Jose, CA, USA).

3.7 Proteomics semiquantification and bioinformatics analysis

PAI is defined as the number of detected peptides divided by the number of detectable peptides per protein[25]. PAI was converted to emPAI[26]. For the detected peptides, SEQUEST counted only the number of unique peptide ions of a protein. Detectable peptides were calculated by an online tool, IPEP (http://ipep.moffitt.org/), subjected to trypsin digestion and detected by electrospray ionization using an ion trap model with two missing cleavages[27]. Biological variability was tested by parallel analysis of three independent biological replicates. Proteins were classified into different functional categories according to the Kyoto Encyclopedia of Genes and Genomes (KEGG) pathway (http://www/genome.jp/kegg/), the OmicsBean database (heep://www/omicsbean.cn) and the UniProt database (http://www/uniprot.org/). All metabolic pathways of *S. spinosa* were drawn with the help of KEGG pathway maps.

3.8 The iTRAQ (isobaric tags for relative and absolute quantitation) protein analysis

The iTRAQ reagent labeled protein samples were trypsinization and lyophilization. The isobaric tagging iTRAQ reagent was added into the protein digest (75% isopropanol) and incubated at room temperature for 2 h. 100 μL water was added into the reaction. The labeled peptide pools were then mixed together and lyophilized. The samples were dissolved in 100 μL of mobile phase A (10 mM ammonium formate, 5% acetonitrile in water, pH=10.0), and the peptide fraction was separated by HPLC (Agilent 1100) with the following conditions: column (ZORBAX Extended-C18), detection wavelength: 215 nm, flow rate: 0.3 mL/min. Separation gradient was a linear gradient from 5 to 38% of Buffer B (10 mM ammonium formate, 90% aqueous acetonitrile, pH=10.0) for 80 min. The eluate solution was collected every minute in the gradient and dried for LC/MS analysis. The SCIEX's ProteinPilot software (v 5.0) was used for database search and protein identification and relative quantitative analysis. The false-positive rate FDR

(False Discovery Rate) was set to 1%. After de-redundancy, trypsin, depth analysis mode (Thorough), mass spectrometry mass error was 20 ppm and mass spectrometry mass error was 0.1 Da.

3.9 RNA extraction and qRT-PCR analysis

Total RNA of *S. spinosa* CCTCC M206084 and *S. spinosa*-Δ*acuC* and *S. spinosa*-*acuC* were separately isolated from broth cultured in TSB medium on the forth day using TRIzol Reagent (Invitrogen). RNA concentration and purification were determined by measuring the ratio of OD260nm to OD280nm. The transcriptional levels of related genes were assayed on 7500 Real-Time PCR system instruments (Applied Biosystems, USA). DNase treatment and cDNA synthesis were performed by PrimeScriptTM RT Reagent Kit with gDNA Eraser (Takara) according to the manufacturer's instructions. The real time qRT-PCR amplification was performed by using SYBR® Permix Ex TagTM GC (Takara). Primer pairs used in qRT-PCR were developed with Primer Premier 5.0 and listed in **Table S2**. PCR was performed at the following conditions: 2 min at 50 °C and 10 min at 95 °C, followed by 40 cycles of 15 s at 95 °C and 1 min at 60 °C. Melting curves were performed from 60 to 95 °C to validate the specificity of PCRs. The 16S rRNA gene was used as an internal control to quantify the relative expression of the target genes.

Statistical analysis

The results were statistically analyzed by SPSS 18.0 and $p < 0.05$ indicated that there was a significant difference between each samples.

Abbreviations

2D-LC-MS/MS: two-dimensional liquid chromatography-tandem mass spectrometry; HPLC: high performance liquid chromatography; iTRAQ: isobaric tags for relative and absolute quantitation; Acs: Acetyl-CoA synthetase; HDAC: histone deacetylase acetylation/deacetylation.

Declarations

Ethics approval and consent to participate

This article does not contain any studies with human participants or animals

by any of the authors.

Consent for publication

Not applicable.

Availability of data and materials

Not applicable.

Competing interests

The authors declare that they have no confict of interest.

Funding

This work was supported by funding from the National Natural Science Foundation of China (31770106), the National Basic Research Program (973) of China (2012CB722301), the Cooperative Innovation Center of Engineering and New Products for Developmental Biology of Hunan Province (20134486).

Authors' contributions

ZDL, JX and JLT designed this study. YL, LS and LC carried out the knockout and overexpression experiments. ZYX extracted the total RNA and performed the HPLC analysis and biological activity assay. ZDL, JR, XZD and LQX designed the study and wrote the manuscript.. All authors read and approved the final manuscript.

Acknowledgements

Not applicable.

References

1. Mertz F P, Yao,R C. *Saccharopolyspora spinosa* sp. nov. Isolated from soil collected in a sugar mill rum still. International Journal of Systematic Bacteriology. 1990, 40(1): 34-39.
2. Thompson, G D, Dutton, R, Sparks, T C. Spinosad – a case study: an example from a natural products discovery programme. Pest Management Science. 2000, 56(8): 696-702.
3. Sparks, T C, Crouse, G D, Durst, G. Natural products as insecticides: the biology, biochemistry and quantitative structure-activity relationships of spinosyns and spinosoids. Pest Management Science, 2001, 57(10): 896-905.
4. Waldron, C, Matsushima, P, Rosteck, P R, Broughton, M C, Baltz, R H. Cloning and analysis of the spinosad biosynthetic gene cluster of *Saccharopolyspora spinosa.* Chemistry and Biology, 2001, 8(5): 487-499.
5. Luo, Y S, Kou, X X, Ding, X Z, Hu, S B, Tang, Y, Xia, L. Q. Promotion of spinosad biosynthesis by chromosomal integration of the Vitreoscilla hemoglobin gene in *Saccharopolyspora spinosa*. Science China Life Science, 2012□55(2): 172-180.
6. Schoonejans, T, Van, S M. Spinosad, a new tool for insect control in vegetables cultivated in greenhouses. Mededelingen, 2001, 66(2a):375-86.
7. Cai, H, Wang, Y, Wan, H, Wang, H, Zhao, Z. Studies on spinosad production of *Saccharopolyspora spinosa.* Chinese Journal of Biotechnology, 2011, 31(2): 124-129.

8. Taunton, J, Hassig, C A, Schreiber, S L. A mammalian histone deacetylase related to the yeast transcriptional regulator Rpd3p. Science, 1996, 272(5260): 408-411.
9. Leipe, D D, Landsman, D. Histone deacetylases, acetoin utilization proteins and acetylpolyamine amidohydrolases are members of an ancient protein superfamily. Nucleic Acids Research, 1997, 25(18):3693.
10. Gregoretti, I V, Lee, Y M, Goodson, H V. Molecular evolution of the histone deacetylase family: functional implications of phylogenetic analysis. Journal of Molecular Biology, 2004, 338(1):17-31.
11. Lombardi, P M, Cole, K E, Dowling, D P. Structure,mechanism,and inhibition of histone deacetylases and related metalloenzymes. Current Opinion in Structural Biology, 2011, 21(6): 735-743.
12. Li, R, Gu, J, Chen, Y Y. CobB regulates *Escherichia coli* chemotaxis by deacetylating the response regulator CheY. Molecular Microbiology, 2010, 76(5):1162-1174.
13. Thao, S, Chen, C S, Zhu, H. Nepsilon-lysine acetylation of a bacterial transcription factor inhibits Its DNA-binding activity. Plos One, 2010, 5(12):e15123.
14. Mikulik, K, Felsberg, J, Kudrnáčová, E. CobB1 deacetylase activity in *Streptomyces coelicolor*. Biochem. Cell Biol, 2012, 90(2):179-187.
15. Dan, H, Li, Z H, Di, Y. Lysine acetylproteome analysis suggests its roles in primary and secondary metabolism in *Saccharopolyspora erythraea.* Applied Microbiology and Biotechnology, 2015, 99(3):1399.
16. Gardner, J G, Grundy, F J, Henkin, T M. Control of acetyl-coenzyme A synthetase (AcsA) activity by acetylation/deacetylation without NAD(+) involvement in *Bacillus subtilis.* Bacteriol, 2006, 188(15):5460-5468.
17. Gardner, J G, Escalante-semerena, J C. Biochemical and Mutational Analyses of AcuA,the acetyltransferase enzyme that Controls the activity of the acetyl-coenzyme a synthetase (AcsA) in *Bacillus subtilis.* Journal of Bacteriology, 2008, 190(14):5132-5136.
18. Tang, Y, Xia, L, Ding, X, Luo, Y, Huang, F,Jiang, Y. Duplication of partial spinosyn biosynthetic gene cluster in *Saccharopolyspora spinosa* enhances spinosyn production. FEMS Microbiol Lett, 2011, 325(1): 22–29.
19. Luo, Y, Ding, X, Xia, L. Conditions for protoplast preparation of spinosyn-producing strain and the physiological properties of protoplast-regenerated strains. Chinese Journal of Bioengineering, 2009, 25(3):360-367.
20. Xie, J Y, Dong, G, Liu, Z. Preparation of Microbial Samples by Scanning Electron Microscopy. Chinese Journal of Electron Microscopy, 2006, 24(4): 440.
21. Yang, Q, Li, Y, Yang, H, Rang, J,Tang, S,He, L. Proteomic insights into metabolic adaptation to deletion of *metE* in *Saccharopolyspora spinosa*. Appl Microbiol Biotechnol, 2015, 99(20):8629-8641.
22. Luo, Y,Ding, X,Xia, L, Huang, F, Li, W, Huang, S. Comparative Proteomic Analysis of *Saccharopolyspora spinosa* SP06081 and PR2 strains reveals the differentially expressed proteins correlated with the increase of spinosad yield. Proteome Sci, 2011, 9(1): 40.

23. Yang, Q, Ding, X Z, Xia, L Q, Liu, S,Sun, Y,Yu, Z. Differential proteomic profiling reveals regulatory proteins and novel links between primary metabolism and spinosad production in *Saccharopolyspora spinosa*. Microbial Cell Factories, 2014, 13(1): 27-43.
24. Huang, S Y, Ding, X Z, Sun, Y J, Yang, Q, Xiao, X Q, Cao, Z P, Xia, L. Q. Proteomic analysis of *Bacillus thuringiensis* at different growth phases by using an automated online two-dimensional liquid chromatography-tandem mass spectrometry strategy. Applied and Environmental Microbiology, 2012, 78(15): 5270-5279.
25. Rappsilber, J U, Ryder, Lamond, M, Mann. Large-scale proteomic analysis of the human spliceosome. Genome Research, 2002, 12(8): 1231-1245.
26. Ishihama, Y, Y Oda, T, Tabata, T, Sato, T, Nagasu, J, Rappsilber. Exponentially modified protein abundance index (emPAI) for estimation of absolute protein amount in proteomics by the number of sequenced peptides per protein. Molecular & Cellular Proteomics, 2005, 4(9): 1265-1272.
27. Lu, D, Liu, R Z, Izumi, V, Fenstermacher, D, Haura, E B, Koomen, J, Eschrich, S A. IPEP: an *in silico* tool to examine proteolytic peptides for mass spectrometry. Bioinformatics, 2008, 24:2801–2802.
28. Detlef, D, Leipe, David, Landsman. Histone deacetylases, acetoin utilization proteins and acetylpolyamine amidohydrolases are members of an ancient proteinsuperfamily. Nucleic Acids Research, 1997, 25(18) :3693–3697.
29. Gardner, J G, Escalantesemerena, J C. In *Bacillus subtilis*, the Sirtuin Protein Deacetylase, Encoded by the srtN Gene (Formerly yhdZ), and Functions Encoded by the acuABC Genes Control the Activity of Acetyl Coenzyme A Synthetase. Journal of Bacteriology, 2009, 191(6):1749-55.
30. Grundy, F J, A, J Turinsky, T, M Henkin. Catabolite regulation of *Bacillus subtilis* acetate and acetoin utilization genes by CcpA. J. Bacteriol, 1994, 176:4527–4533.
31. Gilles, P, Van. Wezel, Jannes, Meulen. ssgA Is Essential for Sporulation of *Streptomyces coelicolor* A3(2) and Affects Hyphal Development by Stimulating Septum Formation, Journal of Bacteriology, 2000, 0021-9193,Vol. 182, No. 20.
32. Lee,Jae-Hyun, Jeong, Haeri, Kim, Younhee, Lee, Heung-Shick. Corynebacterium glutamicum whiA plays roles in cell division, cell envelope formation, and general cell physiology, Antonie van Leeuwenhoek, 2019, s10482-019-01370-9.
33. José, O. Bonilla1, Eduardo, A Callegari, María, C, Estevéz, B Villegas. Intracellular Proteomic Analysis of Streptomyces sp. MC1 When Exposed to Cr(VI) by Gel-Based and Gel-Free Methods. Curr Microbiol, 2020, s00284-019-01790-w.
34. Liu, Y, Sun G, Zhong, Z, Zhang, Yong, Zhou, J, Zheng, X, Deng, K. Overexpression of AtEDT1 promotes root elongation and affects medicinal secondary metabolite biosynthesis in roots of transgenic Salvia miltiorrhiza, Protoplasma, 2016, s00709-016-1045-0.
35. Yoshihiro, Mouri, Kenji, Konishi, Azusa, Fujita, Takeaki, Tezuka, Yasuo Ohnishi. Regulation of Sporangium Formation by BldD in the Rare Actinomycete *Actinoplanes missouriensis*, Journal of Bacteriology, 2017, 199: e00840-16.

36. 36. Maharjan, S, Oh, T J, Lee, H C, Sohng, J K. Heterologous expression of *metK1-sp* and *afsR-sp* in *Streptomyces venezuelae* for the production of pikromycin. Biotechnol Lett. 2008, 30(9), 1621-6.

Tables

Table 1 Biological insecticidal activity of the wild-type and mutant strains

Strains	Relative coefficient（R^2）	LT_{50}(d)	95% Confidence interval
S. spinosa	0.9911	4.093	3.729-4.527
S. spinosa-Δ*acuC*	0.9812	4.534	4.153-5.087
S. spinosa-acuC	0.9877	3.658	3.333-4.036

Table 2 Proteins identified from SDS-PAGE gel analysis

Band number	UniproKB	Protein description	Gene	Theoretical MW (KDa)	Possible function
1	A0A2N3Y983	Tanslation initiation factor IF-2	*inf*B	105.31	Hydrolysis and promotes its binding to the 30S ribosomal subunits. Also involved in the hydrolysis of GTP during the formation of the 70S ribosomal complex.
2	A0A2A3Z889	bifunctional aldehyde dehydrogenase/enoyl-CoA hydratase	*paaZ*	72.0	The oxidoreductase activity, acting on the aldehyde or oxo group of donors, NAD or NADP as acceptor
3	A0A2N3Y9R3	D-3-phosphoglycerate dehydrogenase	*serA*	54.93	This protein is involved in step 1 of the subpathway that synthesizes L-serine from 3-phospho-Dglycerate

Table 3 The types of difference gene related to spinosad biosynthesis

ID	gene	protein name	Fold change	Identity
497996893	*efp*	Elongation factor P	1.53	88.83
498001352	*nusG*	Transcription termination/antitermination protein	1.87	85.71
498001860	*purH*	Bifunctional purine biosynthesis protein	1.56	89.06
498381195	pepB	Group B oligopeptidase	1.61	83.47
497997129	*iolG3*	Inositol 2-dehydrogenase 3	1.65	86.6
498381383	*fabH*	3-oxoacyl-[acyl-carrier-protein] synthase	1.94	83.89
498378866	fabG1	3-oxoacyl-[acyl-carrier-protein] reductase	1.95	88.13
497991096	*atpD*	ATP synthase subunit beta	1.98	96.7
497998623	*fba*	Fructose-bisphosphate aldolase	2.03	91.28
498381238	*nadE*	NH(3)-dependent NAD(+) synthetase	3.03	81.48
498381374	*ahpE*	Alkyl hydroperoxide reductase E	0.31	91.45
497992400	*ftsZ*	Cell division protein	0.38	62.5
497994003	*clpC*	Negative regulator of genetic competence	0.73	91.45

Figures

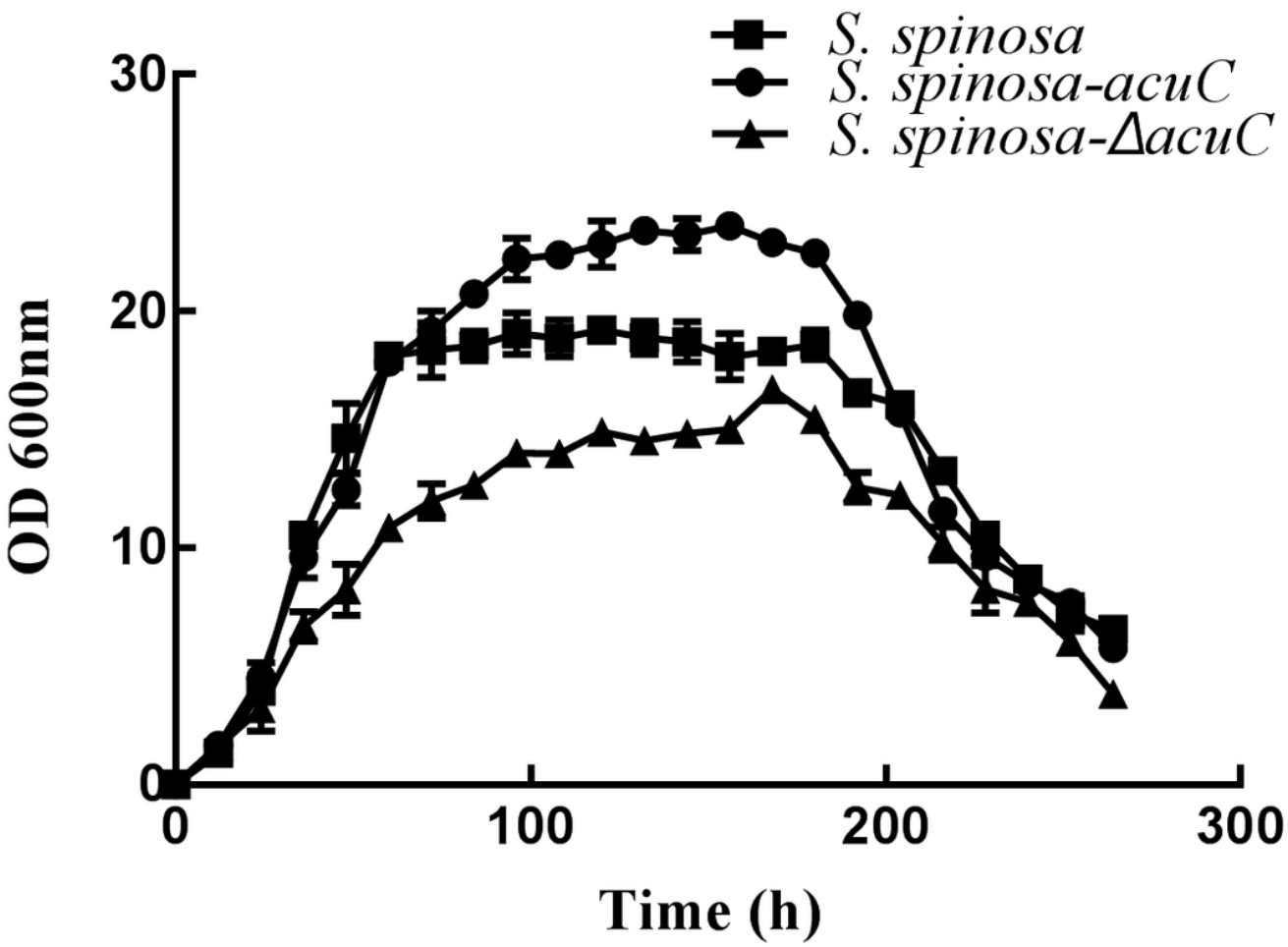

Figure 1

Growth curve of S. spinosa, S. spinosa-ΔacuC and S. spinosa-acuC.

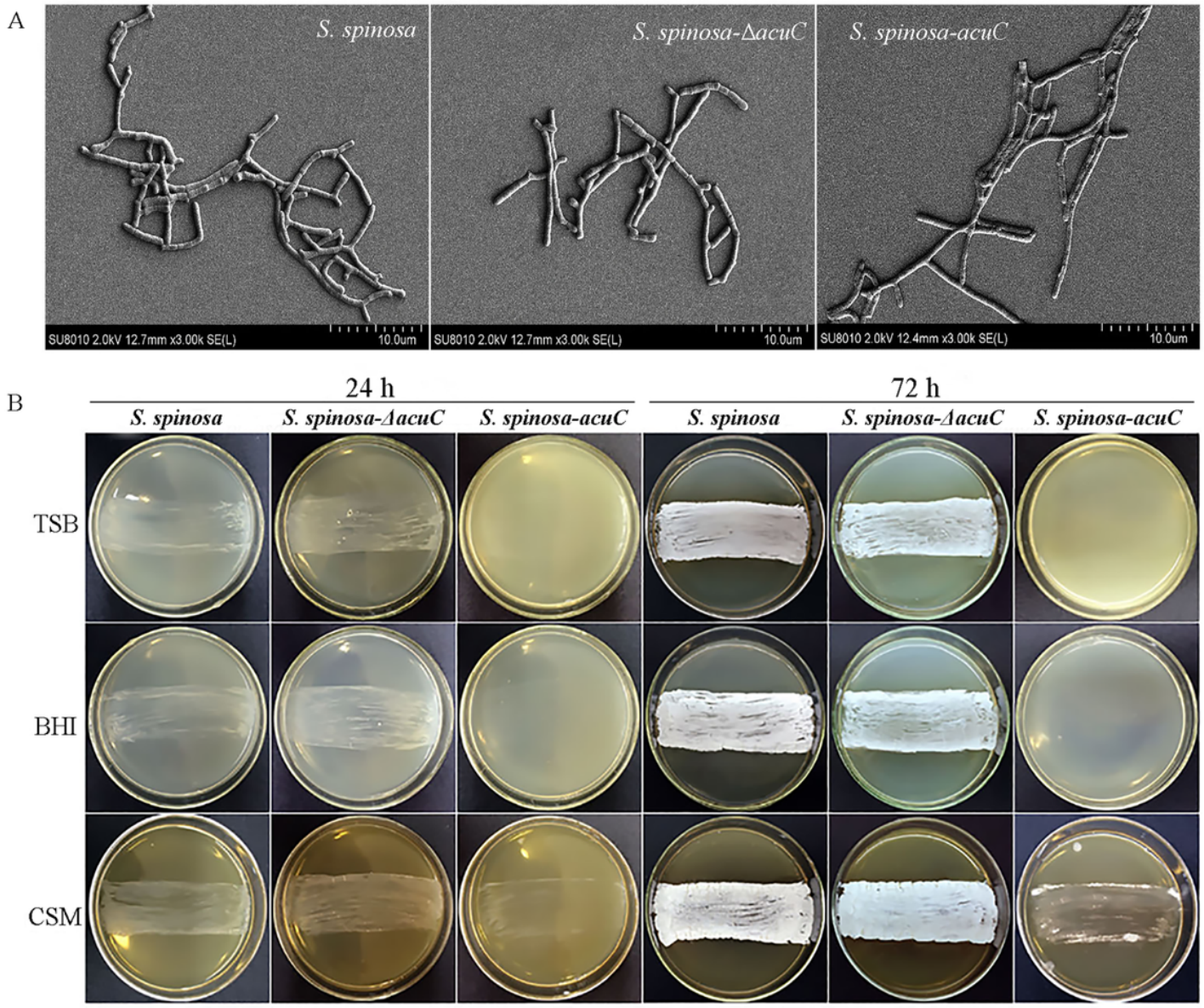

Figure 2

Effects of acuC on the morphology and sporulation of S. spinosa, S. spinosa-ΔacuC and S. spinosa-acuC. A. Scanning electron morphological observation of wild-type and mutant strains after 48 h; B. The morphological comparison of wild-type and mutant strains on different solid media. It was found that the sporulation production capacity of the S. spinosa-ΔacuC and S. spinosa was obviously stronger than S. spinosa-acuC in three culture media. The S. spinosa-acuC produced only a few spores on the CSM medium and almost no spores were produced on TSB and BHI medium.

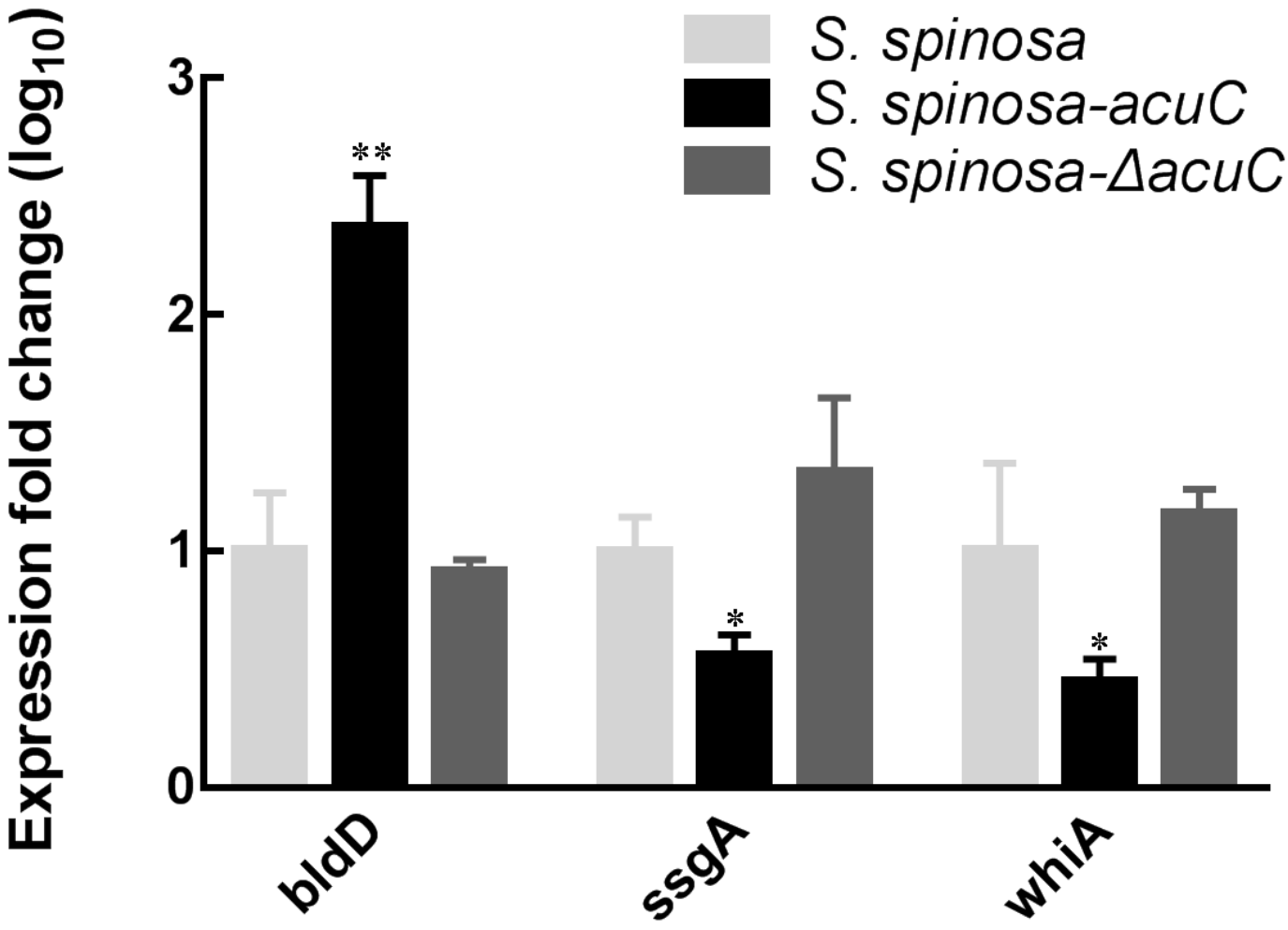

Figure 3

Expression levels of ssgA, whiA and bldD in S. spinosa, S. spinosa-ΔacuC and S. spinosa-acuC. The mRNA samples were isolated from the wild-type and mutant strains on 72 h, the expression of bldD exhibited a significant up-regulated in S. spinosa-acuC, whereas whiA and ssgA was down-regulated. The 16S rRNA gene was used as an internal control to quantify the relative expression of the target genes. Gene expression differences are shown by the bar height. Error bars indicate the standard errors of results from n=3 replicates. *, **and *** indicate $P<0.05$, $P<0.01$ and $P<0.005$, respectively.

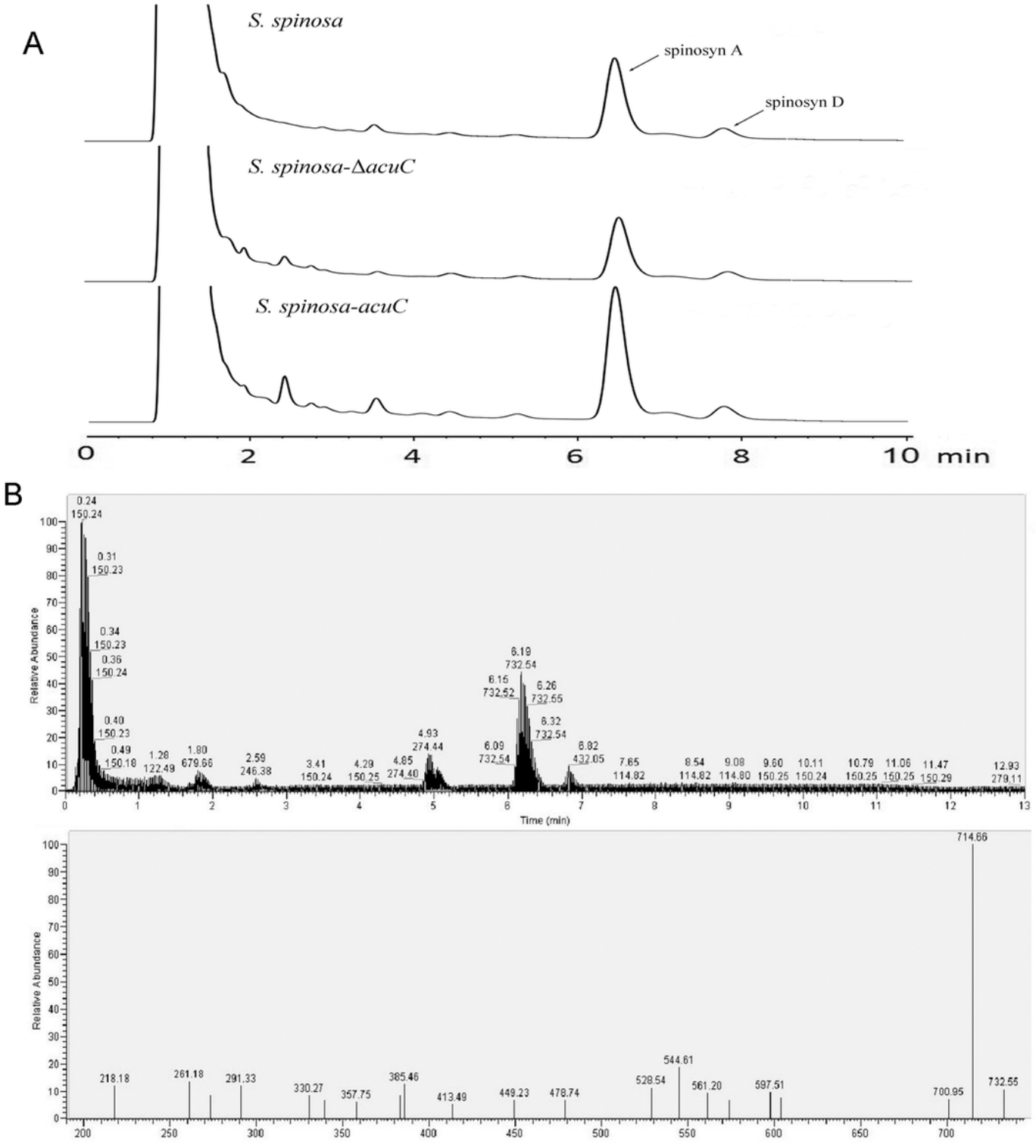

Figure 4

The analysis of the yield of spinosad between the wild-type and mutant strains. A. The HPLC analysis of fermentation yield products of the wild-type and mutant strains; B. The mass spectrometry identification of the target peak.

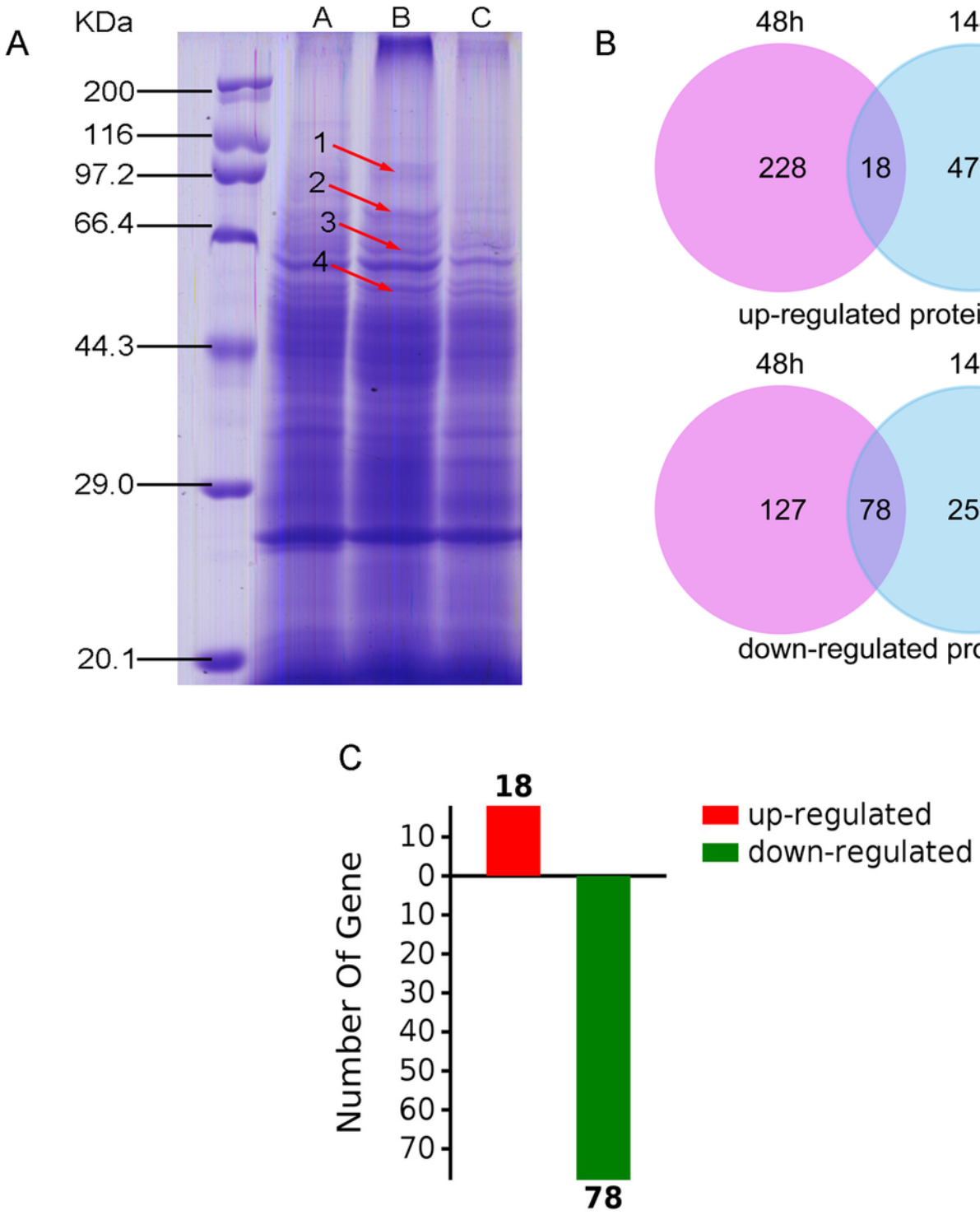

Figure 5

SDS-PAGE analysis and Semi-quantitative proteomic analysis of the wild-type and mutant strains A. The SDS-PAGE analysis of total proteins. (M: Protein marker; A: S. spinosa; B: S. spinosa-acuC; C: S. spinosa-ΔacuC); B. Numbers of the Differential proteins between S. spinosa and S. spinosa-acuC in 48h and 144h; C. The number analysis of up-regulated proteins and down-regulated proteins between S. spinosa and S. spinosa-acuC.

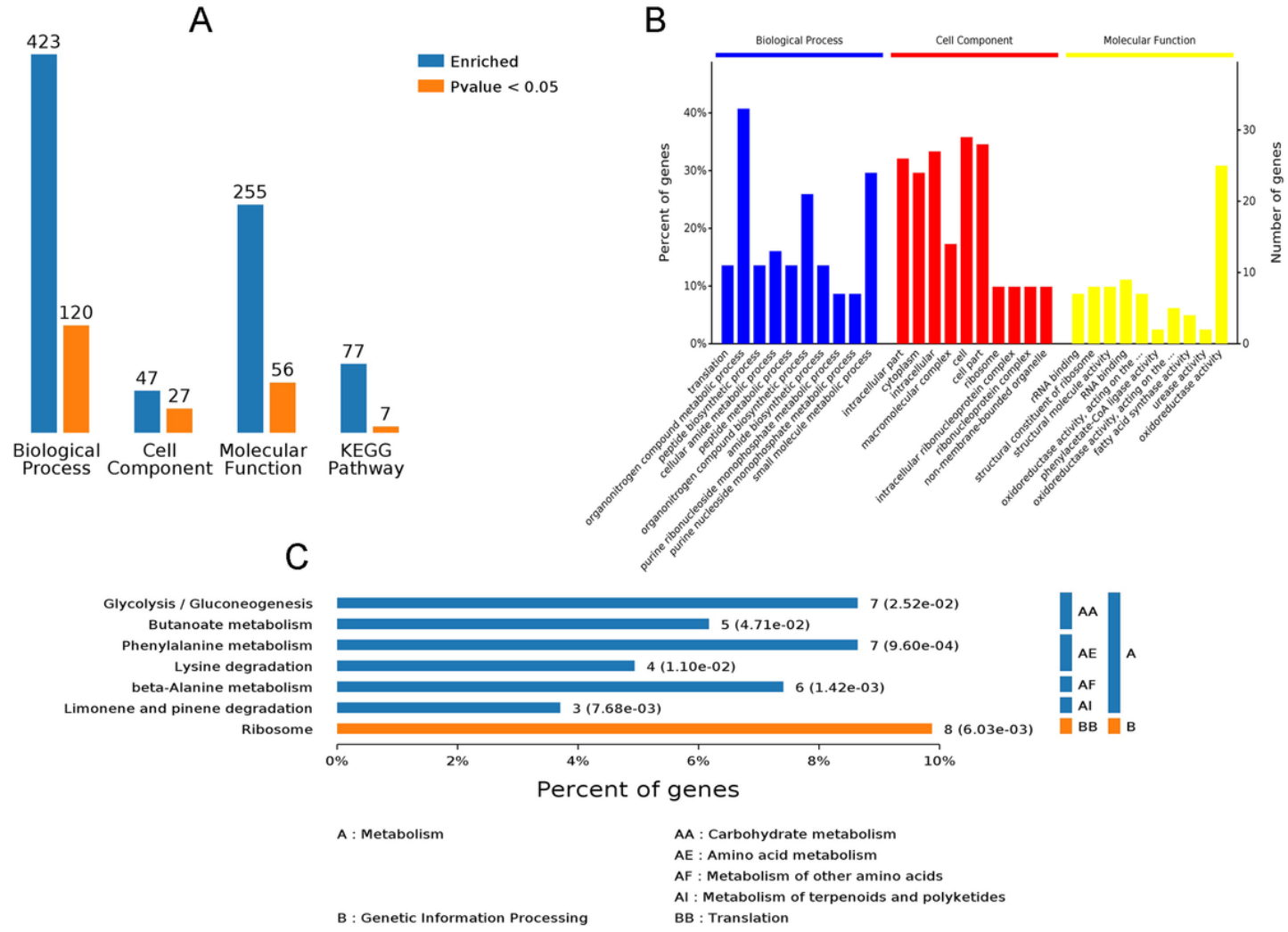

Figure 6

GO enrichment analysis of difference proteins A. The GO enrichment number analysis of proteins; B. The percent statistics of GO enrichment analysis; C. Classes of enriched KEGG Pathway. The GO enrichment analysis and KEGG pathway analysis revealed that significant difference proteins mainly involved in the glycolysis/gluconeogenic, phenylalanine and β-Alanine metabolic pathways.

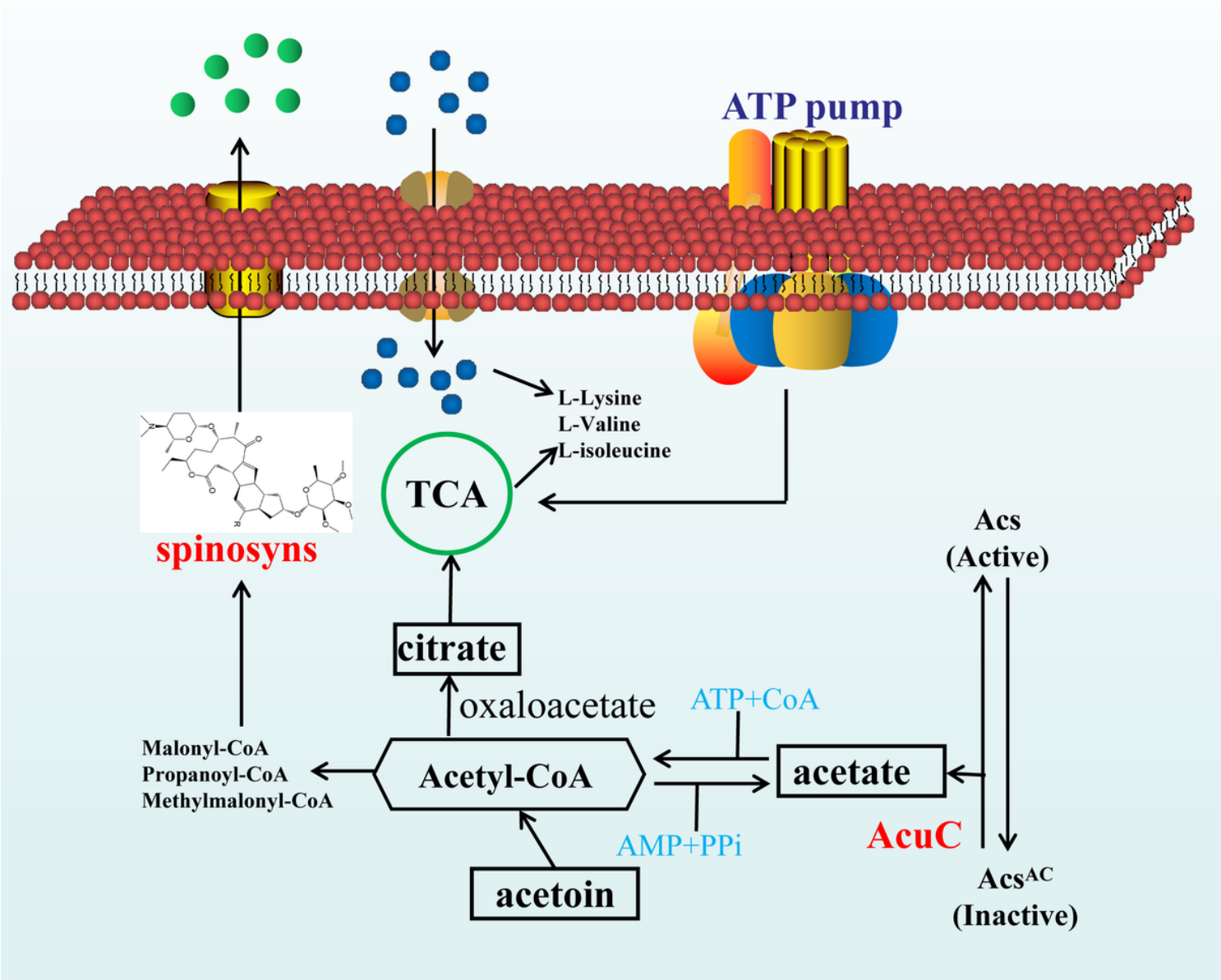

Figure 7

Hypothetical role of AcuC enzyme on acetoin catabolism. The overexpression of the acuC gene activated the acetylated Acs protein and promoted the production of acetate, which further affected the biosynthesis of acetyl-CoA and provided a large number of precursors for spinosad biosynthesis.

Supplementary Files

This is a list of supplementary files associated with this preprint. Click to download.

- Additionalfile.docx